Δt_d, between either line and the reference line is given by the slope of $\Delta\phi$. The insertion phase measured by a microwave network analyzer shows that the slope of delay line 4 is exactly half that of delay line 7. We notice that while the signal to noise ratio of the differential phase was slightly degraded by the high frequency roll-off in the laser modulation response, excellent phase linearity was maintained from 1 to 11 GHz.

REFERENCES

1. H.F. Taylor, Optics News 14, 22, 1988.
2. I.L. Newberg, C.M. Gee, G.D. Thurmond, and H.W. Yen, IEEE MTT-S Digest, 693, 1989.
3. See, for example, IEEE J. of Lightwave Technology, LT-6, special issue on Integrated Optics, 1988.
4. K. Ishida, H. Nakamura, H. Matsumura, T. Kadoi, and H. Inoue, Appl. Phys. Lett. 50, 141, 1987.
5. W. Ng, R. Craig, and H.W. Yen, IEEE J. of Lightwave Technology, LT-7, 560, 1989.

Control of plasmas parameters by ultrashort pulse multiphoton ionization

P.B. Corkum and N.H. Burnett, National Research Council of Canada

Multiphoton ionization has been widely studied because of its implications for atomic and molecular physics. Probably the most active area of current research concerns the energy of the electrons produced as a result of MPI. Experiments have found that electrons can absorb considerably more energy than the minimum required for ionization. The absorption process has become known as above-threshold ionization (or ATI). Strangely, it is rarely noted that the products are plasmas and that a detailed knowledge of both MPI and ATI could be extremely important to plasma physics.

From a plasma perspective, MPI separates the ionization process from electron collisions. The plasmas that are produced are inherently in ionization disequilibrium, with ATI determining the average electron energy (i.e., the temperature). It is also important that plasmas can be created with dimensions much smaller than an electron mean free path.

A simple model of ATI, which is valid if the oscillatory energy of the electron exceeds the ionization potential and the photon energy ($U>I>h\nu$), quantitatively predicts the electron energy. In this long wavelength or high intensity regime, electron tunnelling through the atomic potential barrier can be considered to be a quasi-static process.

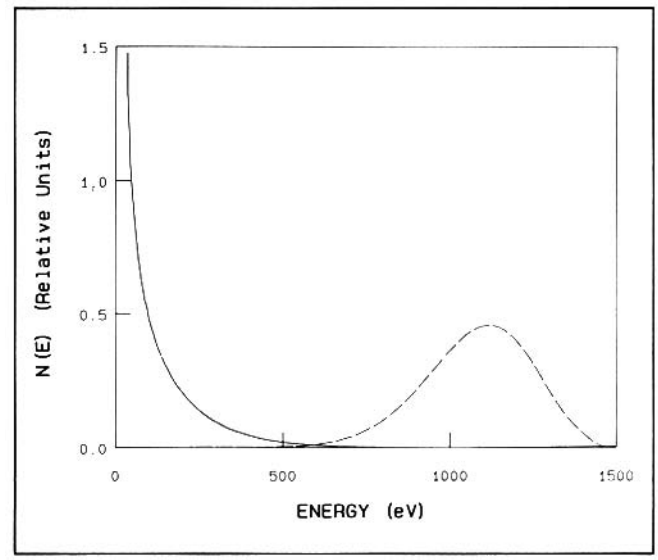

Electron energy distribution for an ionization potential of 12.1 eV. Linearly polarized (solid curve, peak intensity of 10^{14} W/cm^2) and circularly polarized (dashed curve, peak intensity of 2×10^{14} W/cm^2) 10-μm radiation and 2.5-psec pulses were assumed.

Thus, tunnelling formulae predict the probability of ionization as a function of the amplitude and phase of the electric field.

To understand ATI in this limit, consider a newly freed electron. Such an electron can have little energy as it emerges from the barrier, but will gain energy as it subsequently interacts with the external electromagnetic field. By solving the classical equations of motion for linearly polarized light, we find that the electron motion has two components: (1) the oscillatory (or ponderomotive) component is given by $V = q\,E\sin(wt)/mw$ and (2) the drift component is given by $V = q\,E\sin(\Delta\Theta)/mw$, where $\Delta\Theta$ is the phase difference between the phase at which the electron is freed and the peak of the electric field, but the drift component (typical value is about 10% of the ponderomotive energy) remains.

In the quasi-static limit, the probability of ionization as a function of phase is independent of the laser frequency. Thus, the drift energy of the electrons is proportional to w^{-2}. The choice of an excimer or a CO_2 laser as the ionizing laser implied a difference in the electron energy of a factor of about 2000 providing only that the quasi-static limit is respected.

Even more control of the electron temperature can be obtained by simply changing the laser polarization. With circularly polarized light, the drift energy can be shown (still using simple classical physics) to increase by a factor

of about 20. The accompanying figure shows the difference between the ATI electron energy distribution when linearly (solid curve) and circularly (dashed curve) polarized 10 μm light is used to ionize xenon. This additional factor multiplies the 2000 already mentioned. (Furthermore, if the ion species is not of interest, an additional variable is introduced that can add even greater flexibility!)

Although we have emphasized the implications of MPI for electrons, it is clear that ion motion is frozen on the time scale of an ultrashort laser pulse. The plasma density profile will be determined by the initial gas density profile. Thus, like the electron temperature, the ion density is a parameter under experimental control.

One important implication of these results is the production of plasmas for recombination x-ray lasers. If the plasma electron temperature is less than about 10% of the ionization potential, transient inversions are predicted for hydrogen-like or lithium-like ions. Furthermore, the small scale of plasmas that can be produced by MPI is very favorable for all cooling mechanisms and will facilitate quasi-steady state gain on transitions above the resonance level.

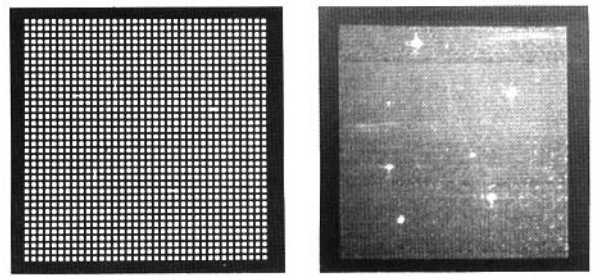

a. b.

Defect size (μm^2)	Coordinates (hor., vert.)
100 × 100	(22, 7.5)
50 × 100	(10, 13.5)
100 × 50	(12.5, 25)
10 × 100	(15, 20.5)
25 × 100	(24, 27.5)
100 × 25	(25.5, 22)
100 × 10	(25.5, 15)

Optical surface inspection using Fourier transform holography in photorefractives.

Real-time enhancement of submicron defects using photorefractives

L. Hesselink, Stanford University

We have developed a new approach using photorefractives for real-time inspection of periodic masks or cracks and defects in non-periodic objects.[1-2] The approach is based on Fourier transform, holographic recording of the object, filtering, and phase-conjugate readout using a photorefractive crystal. These processes are performed simultaneously to allow real-time operation. The object to be inspected (top part of the figure) is placed in the input plane, and the defect-enhanced image in the bottom part appears at the output plane, in a time limited only by the time constant of the photorefractive material. This time constant is material and light intensity dependent and ranges in our experiments from 50 to 250 msecs. This method differs from previous approaches in that all operations are carried out in the Fourier domain, no object dependent mask is needed, and real-time operation is achieved without the need for careful alignment of filters and masks.

The technique for performing real-time defect enhancement is based on two observations. First, the Fourier transform of a periodic object is an array of spikes, whereas the Fourier transform of a small defect is a low amplitude, broad signal. The second observation is that the diffraction efficiency of volume phase holograms formed in a photorefractive medium is maximized when the amplitude of the interfering beams is approximately equal, and decreases as the difference in intensity increases. These observations are used in our apparatus, and defects are enhanced by tuning the amplitude of the reference wave to the amplitude of the weak defect signal. This increases the signal strength of the phase conjugated defect signal relative to the periodic background. As a result, a small spot is visible in the output plane at the defect location, and the periodic pattern has been erased from the image, as shown in the lower part of the figure. Defects ranging from 10 to 100 μm^2 are thus easily located and may be inspected in more detail by subsequent digital or optical processing.

More recently we have extended this approach to include detection of submicron features.[2] As an example, we have detected cracks as small as 0.14 μm in diskheads of magnetic recording devices. The optical signal may be further enhanced by simple digital processing.

REFERENCES

1. E. Ochoa, J.W. Goodman, and L. Hesselink, Real-time enhancement